Aust. J. Phys., 1977, **30**, 379–89

Neutron Resonance Parameters of ^{90}Zr below 300 keV

A. R. de L. Musgrove,[A] *J. A. Harvey*[B] *and W. M. Good*[B]

[A] AAEC Research Establishment, Private Mail Bag, Sutherland, N.S.W. 2232.
[B] Oak Ridge National Laboratory, Oak Ridge, Tennessee 37830, U.S.A.

Abstract

Transmission data taken at both the 80 and 200 m stations of the Oak Ridge Electron Linear Accelerator have provided resonance parameters for ^{90}Zr to 300 keV bombarding energy. The average s-wave parameters obtained were: $\langle D\rangle = 8{\cdot}6\pm1{\cdot}6$ keV and $S_0 = (0{\cdot}54\pm0{\cdot}14)\times10^{-4}$, while the average parameters for the two p-wave sequences were: for $p_{1/2}$, $\langle D\rangle = 8{\cdot}6\pm1{\cdot}6$ keV and $S_1 = (3{\cdot}9\pm1{\cdot}0)\times10^{-4}$; for $p_{3/2}$, $\langle D\rangle = 4{\cdot}3\pm0{\cdot}5$ keV and $S_1 = (4{\cdot}3\pm0{\cdot}8)\times10^{-4}$.

1. Introduction

Recently, Toohey and Jackson (1974) (hereafter TJ) studied the ground state radiative widths of ^{91}Zr by the threshold photoneutron technique. Since the ground state of ^{91}Zr has spin and parity $J^\pi = 5/2^+$, only those p-wave resonances with $J^\pi = 3/2^-$ (i.e. with $g = 2$) were selected by E1 absorption in the reaction. On the other hand, to excite the $p_{1/2}$ resonances would have required M2 absorption probabilities vastly exceeding current theoretical estimates. The photoneutron data, combined with neutron transmission data on ^{90}Zr over the same neutron energy range, provided a nice separation of the observable resonances into the various possible spin and parity classes. To perform quantitative comparisons between their measured radiative widths and the predictions of the valence neutron model of radiative neutron capture, TJ extracted neutron widths in a preliminary analysis of two high resolution transmission measurements performed at the Oak Ridge Electron Linear Accelerator (ORELA). The present paper gives an account of those transmission experiments and extends the early analysis to provide a fairly complete set of resonance parameters below 300 keV bombarding energy. Since TJ were primarily interested in those resonances appearing in ^{91}Zr(γ, n), they did not analyse s-wave widths for many of the resonances observed. Furthermore, the recent analysis by Boldeman *et al.* (1975) (hereafter BAMM) of the ORELA (n, γ) data revealed the presence of many more resonances than had been seen by TJ. We identify many of these as necessarily d wave, and indicate a few cases where TJ have misassigned d-wave resonances (which can decay to the ground state of ^{91}Zr via E2 and M2 radiation) as p-wave resonances with $g = 2$.

2. Experiment and Data Analysis

Two separate transmission runs were performed at ORELA on a metallic zirconium sample enriched to 97·7%, with thickness 0·0827 at. b^{-1}, in ^{90}Zr. The first used a ^{6}Li glass scintillator at the 80 m flight path facility and provided data to

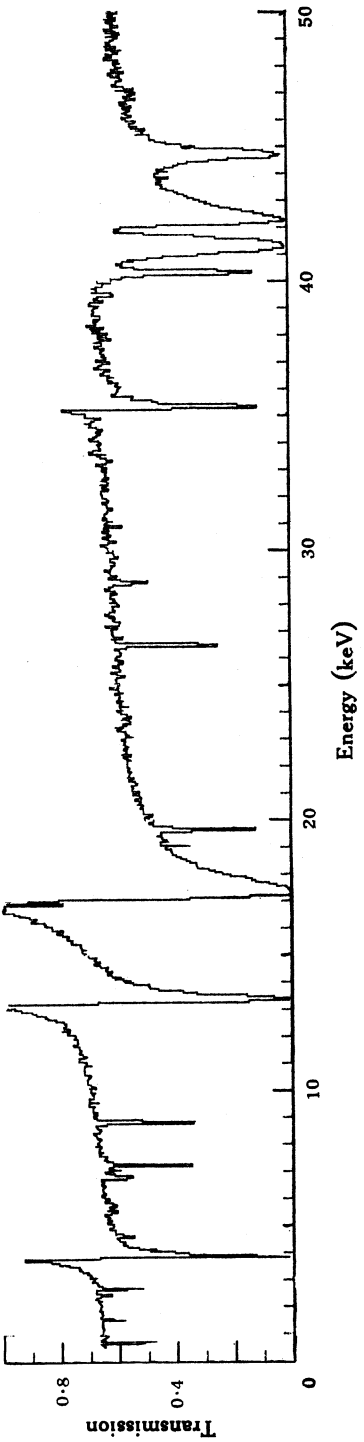

Fig. 1. Transmission data for ^{90}Zr from:
(*below*) the 80 m station (0–50 keV);
(*below opposite*) the 200 m station (50–300 keV).

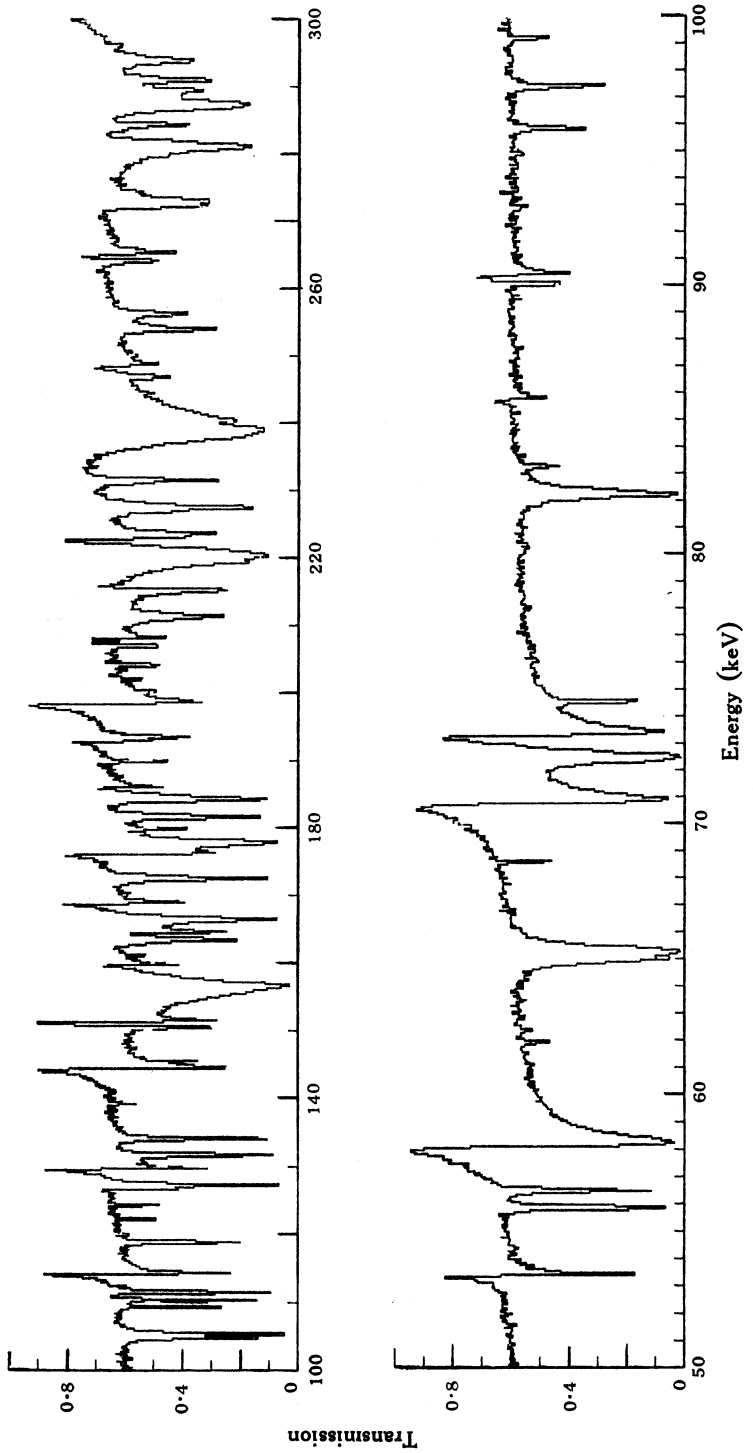
Transmission
0·8
0·4
0
100
140
180
220
260
300
50
60
70
80
90
100
Energy (keV)

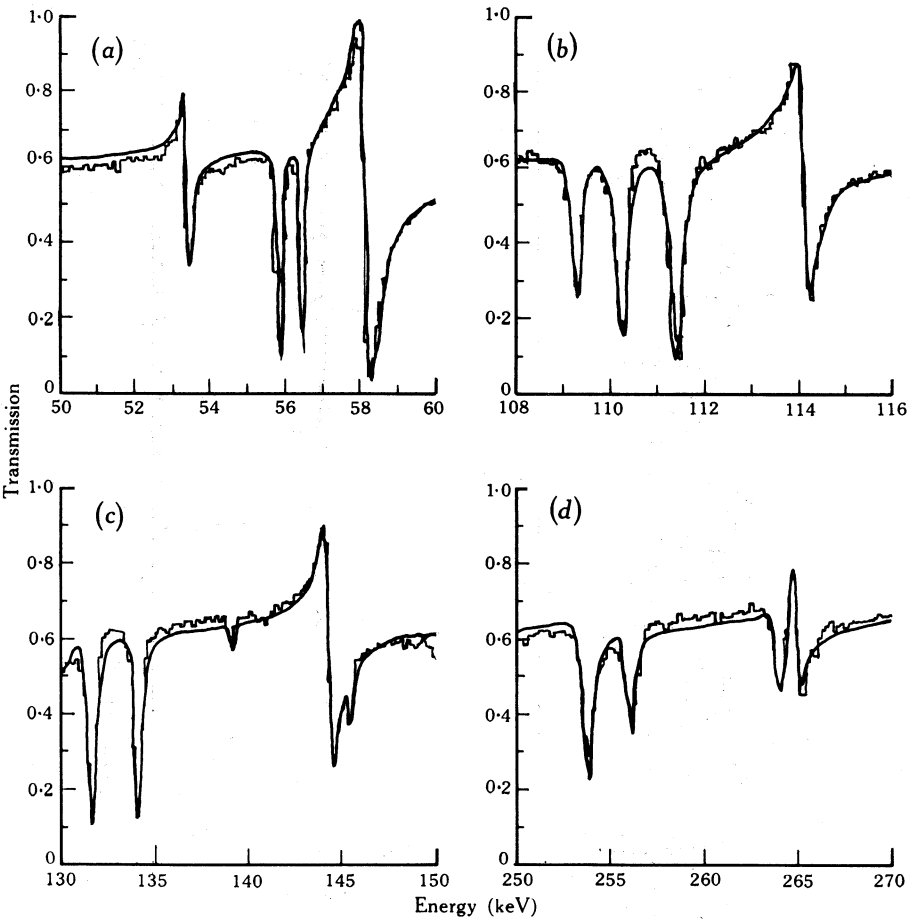

Fig. 2. Representative fits to portions of the ^{90}Zr transmission data.

about 100 keV neutron bombarding energy. The second utilized an NE110 proton recoil counter at the 200 m station to extend the energy range of useful data to $\gtrsim$300 keV. A comparison of the detection efficiencies of the two detectors has been given by Hill *et al.* (1971). Above a few kilovolts the NE110 plastic scintillator is superior in efficiency to ^{6}Li glass by as much as an order of magnitude. For both measurements the neutron burst width was 30 ns. A beam filter of 0·45 g cm^{-2} (0·0027 at. b^{-1}) of ^{10}B eliminated the low energy neutrons from the preceding bursts. Time-of-flight-dependent backgrounds were determined by using 'blacked out' resonances in Cu and Fe (that is, resonances with close to zero transmission in the time region of interest).

The raw data were reduced to transmission form, with appropriate background corrections, dead time corrections and error calculations, using a standard Oak Ridge code. Further details of these procedures have been given by Larson *et al.* (1976). The data were sorted into time channels with widths appropriate to the resolution available in the time region. The area and shape of the transmission dip were then analysed using a nonlinear least squares fitting routine which employed single-level Doppler broadened resonance theory. Usually, less than about 10 resonances were

fitted together, and in this respect our analysis differed from that of TJ, who analysed transmission areas, resonance by resonance, with an approximate correction for nearby resonances. In addition to the area analysis, the exceptionally good resolution ($\Delta E/E \lesssim 0{\cdot}1\%$) allowed the present shape fit to determine g values for the larger p-wave resonances. Neutron widths in excess of $\sim 0{\cdot}0005\,E_n$ gave discernably different transmission profiles. The s-wave resonances were identified by the asymmetry caused by resonance–potential interference.

The transmission data (averaged over many channels) between 0 and 300 keV are shown in Fig. 1, while Fig. 2 gives some examples of calculated fits to restricted regions of the data. The 80 m data were analysed to 60 keV, above which energy the 200 m data had the better statistical accuracy. There is evidence that a multilevel analysis might be required to improve the fit in some regions but, overall, the single-level theory gives good agreement with the experimental data.

3. Results

Table 1 lists the resonances observed in the present data and includes all those previously given by BAMM. Values for $g\Gamma_n$ from the present data are compared with those given by Bartolome *et al.* (1969), TJ and BAMM, and also the evaluated data of Mughabghab and Garber (1973). Resonance energies in parentheses indicate a resonance observed only in capture (BAMM) but not in the present data. For these resonances, a $0{\cdot}2\%$ energy shift was applied, while an asterisk indicates that BAMM could not resolve the neutron width and provided only the quantity $g\Gamma_n\Gamma_\gamma/\Gamma$.

Some of the g values were obtained from the observation (or nonobservation) of the ground state transmissions by TJ; others were provided by BAMM from neutron widths resolved in the capture data. Most are in accord with our shape fit but, because of the implications, the exceptions deserve separate consideration.

40·36 keV Resonance

The 40·36 keV resonance was not well resolved from its $p_{3/2}$ neighbours in the (γ, n) experiment, but it was assigned a large share of the ground state strength. The transmission analysis indicates that this is a $p_{1/2}$ resonance. Incidentally, the total valence width was calculated by BAMM to be several times the measured width; so a $p_{1/2}$ assignment also removes this discrepancy.

99·18 and 100·4 keV Resonances

TJ found a transition to a resonance near 100·4 keV and assigned it to the nearest large resonance visible in transmission: the 99·18 keV resonance. However, BAMM reported a resonance at 100·4 keV in capture and there is also evidence for its presence in the transmission data. This misassignment has been rectified.

110·2 and 111·4 keV Resonances

There is no evidence for the 111·4 keV resonance in the (γ, n) data, whereas the valence model of radiative neutron capture (see e.g. Lynn 1968) would predict a sizeable transition, were it a member of the $p_{3/2}$ sequence. However, the present data are inconsistent with a $g = 1$ assignment for this resonance, and it seems unlikely that so large a resonance, at this energy, could be d wave. Hence a $p_{3/2}$ assignment seems the least unlikely possibility.

Table 1. ^{90}Zr Resonance parameters†

E (keV)	l	g	Γ_n (eV)	$g\Gamma_n$ (eV) obtained from Present	TJ[A]	BAMM[B]	BHMTB[C]	MG[D]
3·855±0·010	0		11·36±0·15	11·36	9·7	10	9·6	11
4·005±0·005	1			0·19±0·05	0·5		0·16	
7·251±0·005	1	2	2·95±0·25	5·90	5·8	8	8·8	8·4
8·852±0·005	1	1	5·50±0·35	5·50	5·8	6	6·5	7·3
9·591±0·005	1			0·035±0·025	—	0·015		0·086
(12·215)				<0·03	—	0·035	0·27	
13·365±0·015	0		65±5	65	51·6	84	76	70
16·888±0·008	1			0·76±0·25	1·7			
(16·965)						0·019		
17·313±0·015	0		202±8	202	195·2	190	230	210
19·085±0·010	1			0·70±0·10	9·0	~9		
19·685±0·010	1	(1)	12·5±0·5	12·5	31·5	22·5		
26·470±0·015	1	2	1·3±0·1	2·6	7·2			
26·530±0·015	1	1	11·3±0·5	11·3	14·6	15		
28·810±0·015	1	2	0·75±0·25	1·5	2·4			
35·34±0·02	0		39±2	39	68·7	⩽18		89
39·52±0·02	1	2	1·6±0·2	3·2	2·4			
40·36±0·02	1	1[E]	60±2	60	62·6	100[F]		94
41·34±0·03	1	2	209±10	418	390	520		362
42·25±0·03	0		250±10	250	278·7	~260		342
44·70±0·03	1	2	88±4	176	146·4	100		320
53·38±0·03	0		23±3	23	18·3	—		
55·83±0·03	1	1	67±5	67	61·2	~60		126
56·43±0·03	1	(1)		48±4	36·5			
58·18±0·04	0		212±10	212	325			310
61·86±0·04	1	2	1·8±0·5	3·6	1·4			
62·40±0·05	1			1·0±0·5				
64·96±0·05	1	1[G]	127±5	127	129·6			
65·22±0·05	1	2	135±5	270	232·6			
68·54±0·05	1	2	5·0±0·5	10	2·0	50		
70·84±0·08	0		230±25	230	147·4			
72·42±0·05	1	2	155±10	310	288·8			
73·33±0·05	0		150±10	150	289			
74·49±0·05	1	2	25±4	50	27·4			
75·52±0·05	(1)			2±1	—	*		
76·00±0·05	(2)			1·5±1	—	*		
79·68±0·05	(2)			0·5±0·5	—	*		
80·16±0·05	(2)			0·5±0·5	—	*		
(81·48)				—	—	*		
82·16±0·05	1	2	99±5	198	209·2	240		
83·23±0·05	1	(1)		14±3	—			
85·73±0·05	0		6·5±1·0	6·5	25			
(85·5)				—	—	*		
90·01±0·05	1			18±2	—	—		
90·37±0·05	0		19±3					
92·89±0·05	1	2	2·0±0·7	4±1	5·0			
94·30±0·05				2±1	—	*		
94·82±0·05				4±1	—	—		
95·78±0·05	1	2	17·5±2·0	35±4	15·6			

† For notes, see end of table.

Table 1 (*Continued*)

E (keV)	l	g	Γ_n (eV)	$g\Gamma_n$ (eV) from Present	TJ[A]	BAMM[B]
96·50±0·05	(2)			~0·75	—	*
97·34±0·95	1	2	23±2	46	35·4	
99·18±0·05	(1)	(1)[H]		9·3±10	5·0	
100·4±0·1	(1)	(2)[H]		2±1	—	*
104·7±0·1	1	1[E]	210±15	210	237·5	240
105·2±0·1	1	2	150±7	300	244·8	
(180·2)	(2)			<0·5	—	*
109·2±0·1	1	2	58±7	116	99·6	
110·2±0·1	1	2	81±7	162	132	
111·4±0·1	1	2[E]	119±10	238	245	
112·3±0·1	(2)			2±1	—	*
114·1±0·1	0		136±12	136	124	
(118·5)	(2)					*
118·8±0·1	1	1[E]	142±7	142	119·2	
121·5±0·1	(2)			<3	—	*
122·2±0·1	(1)			23±3	—	*
(122·4)	(2)					*
124·2±0·1	(1)			26±3	32·5	
126·7±0·1	(2)			34±5	{ 432·6	
127·2±0·1	1	2	213±15	426		
(128·0)	(2)			—	—	*
129·6±0·1	0		139±10	139	91·3	
(130·1)	(2)			—	—	*
(130·6)	(2)			—	—	*
131·6±0·1	1	2[E]	171±8	342	352·9	~350
(133·4)	(2)			—	—	*
134·1±0·1	1	2	167±7	334	276	
139·1±0·1	1	2	7±1	14	16·4	
144·3±0·1	0		325±15	325	70·6	
145·4±0·1	(2)			29±3	—	*
(146·9)	(2)					*
148·3±0·1	(2)			3±2	—	*
150·3±0·1	1	1	190±15	190	106·5	
151·2±0·1	0		225±25	225	*	~300
155·6±0·5	1	1	1900±250	1900	{ 2440	
156·6±0·5	1	2	360±30	720		
159·7±0·1	0		49±6	49	*	
160·0±0·1	(2)			10±5	—	*
161·1±0·1	(1)	(2)		42±5	—	*
163·3±0·1	1	(1)[E,I]	1090±200	1090	481	
164·3±0·1	0		350±50	350	*	
166·3±0·1	1	2	430±30	860	880	
168·8±0·1	0		130±20	130	*	
172·4±0·1	1	2	300±25	600	533	
176·1±0·1	1		170±20	170	*	
177·6±0·1	1	2	875±150	1750	1160	
179·8±0·1	(1)	(1)	89±9	89	93	
181·5±0·1	1	2	272±20	544	525	
184·3±0·1	1	2	410±30	820	776	
186·0±0·1	0		50±7	50	*	

Table 1 (*Continued*)

E (keV)	l	g	Γ_n (eV)	$g\Gamma_n$ (eV) from Present	TJ[A]	BAMM[B]
(188·0)	(2)			—	—	*
189·9±0·1	1	1[E]	78±8	78	141	
192·8±0·1	0		92±10	92		
193·4±0·1	1	1	106±10	106		
198·4±0·1	0		470±30	470		
200·0±0·1				30±10		
201·8±0·1				10±5		
204·0±0·1				50±10		
206·8±0·1				67±10		
207·8±0·1				24±10		
208·1±0·1	0		96±10	96		
211·1±0·2	1	2	650±100	1300	510	
215·0±0·2	1	2	375±70		405	
219·2±0·3	1	1	2400±300	2400	2620	
220·3±0·3	1	2	755±75	1510		
222·8±0·3	0		345±35			
223·6±0·3	(1)	(2)		160±20		
227·3±0·2	1	2	466±50			
231·2±0·2	1	1	413±45			
238·1±0·5	1	2	1500±150			
240·0±0·5	1	1	3250±300			
244·4±0·2				42±6		
246·7±0·2				164±20		
248·5±0·2	0		96±10			
253·8±0·2	1	2	290±25			
256·0±0·2	1	1	300±30			
264·0±0·2	1	1	200±20			
264·9±0·2	0		170±25			
272·3±0·3	1	2	550±50			
272·7±0·3	0		290±30			
280·7±0·3	(1)	(2)	1095±150			
284·1±0·3				360±50		
287·1±0·3	1	2	1070±100			
289·4±0·3	1	2	240±40			
290·9±0·3				420±50		
293·7±0·3	1	2	246±30			
300·9±0·3	0		410±50			

[A] TJ, Toohey and Jackson (1974). An asterisk denotes an s-wave resonance not analysed by TJ, while a dash denotes a weak resonance not analysed by TJ.

[B] BAMM, Boldeman *et al.* (1975). An asterisk denotes that BAMM could not resolve the neutron width and they provided only the quantity $g\Gamma_n\Gamma_\gamma/\Gamma$. A dash denotes a weak resonance not analysed by BAMM.

[C] BHMTB, Bartolome *et al.* (1969).

[D] MG, Mughabghab and Garber (1973).

[E] Note change from g value of TJ, based on shape fit to present data.

[F] BAMM measured $\Gamma_n = 50\pm30$ but assumed $g = 2$.

[G] BAMM gave $g = 2$ for this level from their shape fit.

[H] 99 keV incorrectly assigned $g = 2$ by TJ. They saw the 100·4 keV resonance.

[I] TJ misassigned this as the 161·1 keV resonance.

118·8 keV Resonance

Moderate transitions from the ground state to the 118·8 keV resonance led TJ to assign it to the $p_{3/2}$ sequence. Fig. 3 shows the alternative fits to the transmission dip for $g = 1$ and 2, which clearly favour a $p_{1/2}$ assignment. Since this would imply an anomalously strong M2 transition, it seems more likely that the weak capture resonance located at 118·5 keV is d wave, and is responsible for the ground state line observed.

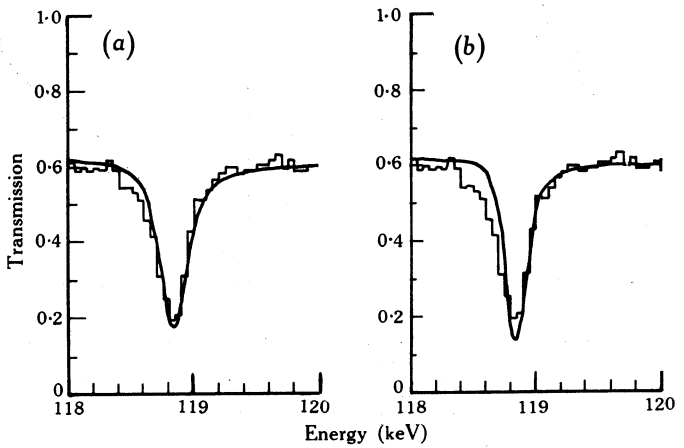

Fig. 3. Fits to the 118·8 keV resonance assuming (*a*) $g = 1$ ($\Gamma_n = 140$ eV) and (*b*) $g = 2$ ($\Gamma_n = 68$ eV).

131·6 keV Resonance

No ground state transitions were observed by TJ to either the 131·6 keV state or to any of the small neighbouring resonances detected in capture. Nevertheless, a $g = 1$ assignment is inconsistent with the data.

4. Average Resonance Parameters

In Figs 4*a*–4*c* the cumulative level count and cumulative sum of reduced neutron widths (calculated using penetrability radius $R = 6{\cdot}07$ fm) are superimposed and plotted against neutron energy for $s_{1/2}$, $p_{1/2}$ and $p_{3/2}$ resonances respectively. The average level spacings and strength functions obtained from the best straight line fits to the slopes of these plots are:

Quantity	Value for $l, J^\pi =$	$0, 1/2^+$	$1, 1/2^-$	$1, 3/2^-$	$2, —$
$\langle D \rangle$ (keV)		8·6 ±1·6	8·6 ±1·6	4·3 ±0·5	—
$10^4 S_l$		0·54 ±0·14	3·9 ±1·0	4·3 ±0·8	0·4 ±0·2

In Fig. 4*d* the remaining resonances (mostly weak) have been analysed assuming that they are d wave. Several of the larger d-wave neutron widths have been obtained from the transmission data while, for others, an estimate of approximately half the detectability limit was used. The d-wave strength function obtained is comparable with the s-wave strength function and indicates that the assignment of these weak resonances as d wave is plausible.

For the s- and p-wave sequences, the level densities are found to be parity independent and proportional to the usual $2J+1$ factor, within experimental uncertainties. Several resonances are missed (or are unable to be assigned) above about 200 keV.

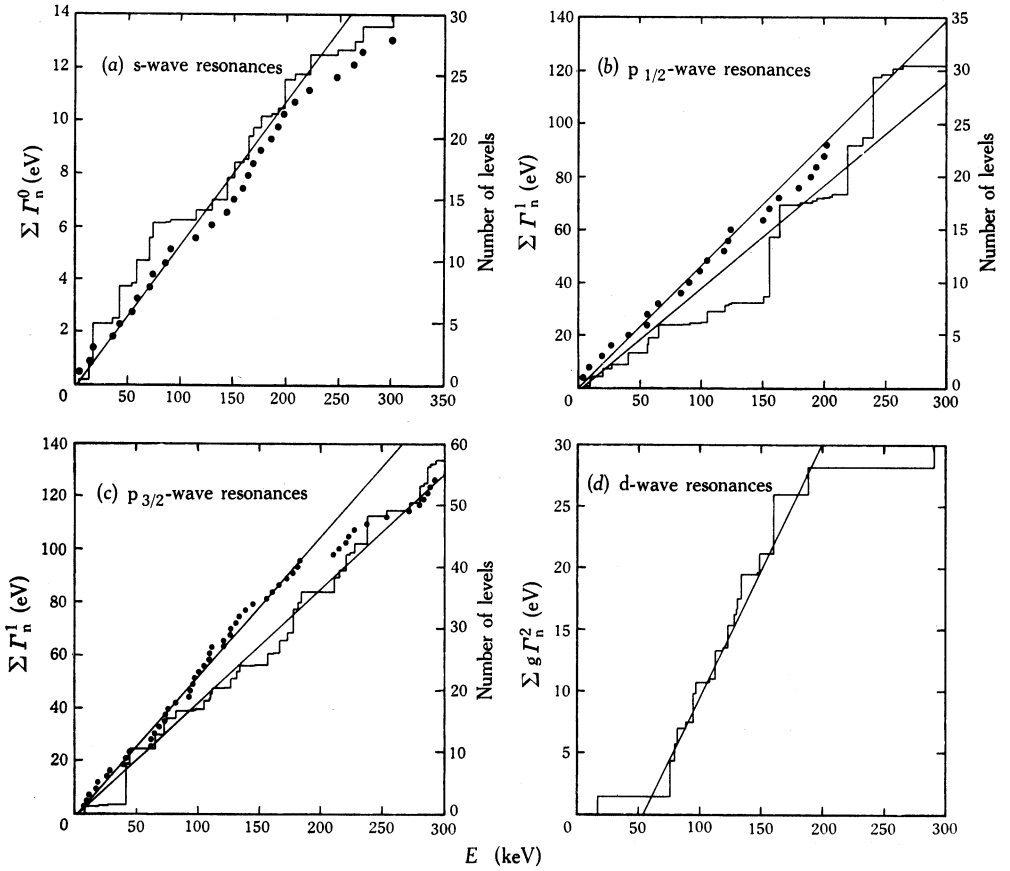

Fig. 4. Plots for the indicated resonances of:

(*a*)–(*c*) The cumulative reduced neutron widths $\sum \Gamma_n^l$ (staircase) and the number of levels N (points) observed below energy E. The best straight line fits to the points and staircase are shown; they are collinear in (*a*). These lines provide respectively the estimates of the neutron strength function and the average level spacing tabulated in Section 4.

(*d*) The quantity $\sum g\Gamma_n^2$ below energy E. This plot is for the weak resonances not assigned to the above classes and assumed to be d wave. The straight line of best fit provides an estimate of the d-wave neutron strength function tabulated in Section 4.

While the energy range covered in the present analysis is of the same order as the spreading widths expected for intermediate structure caused by pre-equilibrium interactions, no feature of any of the present plots gives any suggestion of energy-dependent structure. This is in contrast with both radiative and neutron widths in the neighbouring nuclei of ^{88}Sr and ^{92}Zr (Boldeman *et al.* 1976*a*, 1976*b*) which indicated the presence of such structure.

Finally, we note that with the altered g assignments in the present data, the reported disparity between $p_{3/2}$ and $p_{1/2}$ neutron strength functions (BAMM) has all but disappeared (within the statistical uncertainty).

Acknowledgment

This work is sponsored in part by ERDA under contract to Union Carbide Corp.

References

Bartolome, Z. M., Hockenbury, R. W., Moyer, W. R., Tatarczuk, J. R., and Block, R. C. (1969). *Nucl. Sci. Eng.* **37**, 137.

Boldeman, J. W., Allen, B. J., Musgrove, A. R. de L., and Macklin, R. L. (1975). *Nucl. Phys.* A **246**, 1.

Boldeman, J. W., Allen, B. J., Musgrove, A. R. de L., Macklin, R. L., and Winters, R. R. (1976*a*). *Nucl. Phys.* A **269**, 31.

Boldeman, J. W., Musgrove, A. R. de L., Allen, B. J., Harvey, J. A., and Macklin, R. L. (1976*b*). *Nucl. Phys.* A **269**, 397.

Hill, N. W., Harvey, J. A., Slaughter, G. G., and St. James, A. (1971). Oak Ridge Natl Lab. Progr. Rep. No. ORNL-4743, p. 137.

Larson, D. C., Harvey, J. A., and Hill, N. W. (1976). Oak Ridge Natl Lab. Rep. No. ORNL/TM5612.

Lynn, J. E. (1968). 'Theory of Neutron Resonance Reactions' (Clarendon: Oxford).

Mughabghab, S. F., and Garber, D. I. (1973). Brookhaven Natl Lab. Rep. No. BNL-325, 3rd Ed., Vol. 1.

Toohey, R. E., and Jackson, H. E. (1974). *Phys. Rev.* C **9**, 346.

Manuscript received 24 November 1976